Available online at www.sciencedirect.com
SCIENCE DIRECT®
PERGAMON
Applied Geochemistry 18 (2003) 1165–1184
Applied Geochemistry
www.elsevier.com/locate/apgeochem

Thermodynamic stability of waste glasses compared to leaching behaviour

Didier Perret[a,*], Jean-Louis Crovisier[b], Peter Stille[b], Graham Shields[b,1], Urs Mäder[c], Thierry Advocat[d], Kaarina Schenk[e], Marc Chardonnens[e]

[a]*Ecole Polytechnique Fédérale de Lausanne, Institut des Sciences et Technologies de l'Environnement, Laboratoire de Pédologie, CH-1015 Lausanne, Switzerland*
[b]*ULP Ecole et Observatoire des Sciences de la Terre CNRS, Centre de Géochimie de la Surface UMR 7517, 1, Blessig, F-67084 Strasbourg Cedex, France*
[c]*Universität Bern, Mineralogisch-Petrographisches Institut, 1, Balzerstrasse, CH-3012 Bern, Switzerland*
[d]*CEA Marcoule, Service de Confinement des Déchets, BP 171, F-30207 Bagnols sur Cèze Cedex, France*
[e]*Swiss Agency for Environment, Forests and Landscape, Division Waste, CH-3003 Bern, Switzerland*

Received 10 January 2002; accepted 5 November 2002
Editorial handling by J.-C. Petit

Abstract

The thermodynamic stability of products obtained from the high-temperature treatment of municipal solid wastes and their associated residues (bottom ash, fly ash, filter cake, optional additives) can be estimated by calculation of their free energy of hydration ΔG_{hydr} by a polyhedral approach. This approach has been applied on a series of 23 samples originating from high-temperature treatment processes operated under a range of conditions, and 3 thoroughly characterised standards. For vitreous or vitrocrystalline samples, it is demonstrated that Si and Ca contents clearly control their thermodynamic stability, and that the type of incineration process plays only a minor role. Silicon directly influences the durability of the samples, while Ca governs the pH during corrosion, which in turn affects the thermodynamic stability. It is also shown that there is a tight inverse relationship between the calculated thermodynamic stability of the samples and their rates of dissolution under aggressive conditions of corrosion. Attempts to compare the results to the large literature database of results obtained from nuclear high-level waste glasses, their proxies and other analogs (ancient and commercial glasses) are limited by sample preparation constraints. It is however concluded that the calculated thermodynamic stability of these "waste glasses" offers a valid estimate for their relative quality and, in turn, for their durability.
© 2003 Elsevier Science Ltd. All rights reserved.

1. Introduction

The assessment of the long-term stability of man-made materials has a long history, which has been mostly based on the results of experiments that attempt to accelerate, either chemically or physically, the corrosion of the materials of interest. In the field of glasses and vitreous materials, the seminal work of Paul and Newton (Paul, 1977, 1982; Newton and Paul, 1980; Newton, 1985) on the thermodynamics of hydration of glasses opened up new opportunities in the estimation of their durability. Their conceptual model is that the structure of a glass is an homogeneous assembly of silicate polyhedra of the different elements present in the glass.

According to the theory of Paul and Newton, a glass which is subjected to water corrosion will hydrate with respect to its overall thermodynamic characteristics. Thus, assuming an assembly of silicate polyhedra, the

* Corresponding author. Fax: +41-21-6935-670.
E-mail address: didier.perret@epfl.ch (D. Perret).
[1] Present address: School of Earth Sciences, James Cook University, Townsville, Queensland 4811, Australia.

0883-2927/03/$ - see front matter © 2003 Elsevier Science Ltd. All rights reserved.
doi:10.1016/S0883-2927(02)00245-7

overall free energy of hydration ΔG_{hydr} of a glass can be estimated as the molar-weighted sum of the free energies of hydration $\Delta G_{hydr(i)}$ of the constituent silicates.

This concept was later revisited and refined by Jantzen, Plodinec and Wicks (Jantzen, 1984, 1988; Plodinec, 1984; Jantzen and Plodinec, 1984; Plodinec and Wicks, 1994), who used it to predict the stability of radioactive waste glasses (nuclear high-level waste glasses, HLW glasses). Additionally, Jantzen and Plodinec observed that there is a fairly good relationship between the calculated free energy of hydration of several glasses (HLW, commercial, ancient and natural glasses) and the release of major elements during corrosion tests performed under well defined conditions.

The thermodynamic approach of the free energy of hydration is based on simplifying assumptions and restrictive conditions, i.e. the release of species from the glass matrix is a congruent process far from equilibrium, no secondary products form at the surface of the glass, and there is no geometric or mechanical effect on glass corrosion. This approach has proven very adequate when dealing with glasses containing hazardous elements which must be stored in deep geological repositories (e.g., HLW glasses; Bates et al., 1994; Ewing, 1996).

It is generally considered that, after initiation of the reaction by an acidic ion-exchange mechanism, glass corrosion proceeds via alkaline dissolution and hydrolysis of the external and internal siloxane groups (Scholze, 1991; Grambow and Müller, 2001; Oelkers, 2001; Oelkers and Gislason, 2001), as given by reactions 1 and 2:

$$\left\{\equiv Si - O - Si(OH)_3\right\}_{glass} + OH^- \longrightarrow$$

$$\{\equiv Si - O^-\}_{glass} + H_4SiO_4 \text{(external glass dissolution)} \quad \text{(reaction 1)}$$

$$\{\equiv Si{-}O{-}Si \equiv\}_{glass} + OH^- \longrightarrow$$

$$\{\equiv Si{-}O^-\}_{glass} + \{HO{-}Si \equiv\}_{glass} \text{(internal glass hydrolysis)} \quad \text{(reaction 2)}$$

The thermodynamic model is in agreement with these mechanisms; it represents a simple and sound complementary approach which has been used successfully to estimate the durability of HLW glasses. The present study is part of a two-year project initiated by the Swiss Agency for Environment, Forests and Landscape (SAEFL, 1996, 1998) to estimate the ecological feasibility of reuse for civil engineering applications of vitreous products originating from the high-temperature treatment of municipal solid wastes or their residues (hereafter referred to as waste glasses; Perret et al., 2000) or their landfill disposal.

It is the first attempt to apply the thermodynamic concept of free energy of hydration to a large set of waste glasses obtained from the high-temperature treatment of municipal solid wastes (MSW) or their associated residues (bottom ash, BA; fly ash, FA; filter cake, FC) under various conditions of operation, and to compare their calculated thermodynamic stability to the results of an experimental leaching test performed under drastic conditions of corrosion.

Although the approach adopted in this study allows a comparative evaluation of the performances of the samples, the estimation of the expected long-term behaviour of waste glasses on the basis of short-term corrosion experiments must be viewed with great care because the long-term rate relies on additional parameters (e.g., formation of secondary phases).

2. Materials and methods

2.1. Samples and standards

Table 1 gives an overview of the 23 samples and 3 standards used in this study. The samples are classified according to the category of process from which they were prepared: in-line processes produce waste glasses from the direct high-temperature treatment of MSW, while post-processes yield waste glasses from the high-temperature treatment of incineration residues (BA, FA, FC, or a combination of these residues, with possible additives, e.g., sewage sludge, cement, recycled glass or car shredder residues). The 23 samples were provided by 10 Swiss, German and French companies active in the thermal treatment of MSW or their residues. On the basis of their amount of crystalline components, vitreous and vitrocrystalline samples are distinguished: vitrocrystalline samples contain more than ca. 2% of crystalline phases and are labelled with an asterisk (e.g., sample P2*, standard R2bis*).

According to the companies participating in this study, the samples are representative of normal operating conditions of their high-temperature process, while composition of the input material (i.e., MSW, BA, FA, FC, additives) was typical. The variability of the waste glasses (e.g., differences in the quality of MSW, BA, FA, FC between Switzerland, Germany and France, or between the periods of production) was not addressed in this study, but it is expected to account only for minor variations in the final characteristics of the waste glasses.

Three additional glasses were used in this study for comparative and normalisation purposes. The first of them, SON68, is the non-radioactive proxy of the extensively characterised French nuclear HLW glass R7T7 (Nogues, 1984; Fillet, 1987; Advocat, 1991; Cheron et al., 1995). Although the composition of this borosilicate glass, which is constant from batch to batch, deviates from the average of the 23 samples, it

Table 1
Overview of the 23 samples and 3 standards

Code	Process category	Input material	Process type and temperature
P1	In-line process for MSW	100% MSW	Pre-heating of MSW at 600 °C, then melting in burner at 2000 °C
P2*	In-line process for MSW	100% MSW	Pre-combustion of MSW, then melting in rotative oven at 1350–1450 °C
P3*	In-line process for MSW	100% MSW	Pre-treatment of MSW in fluidised bed at 500–600 °C, then melting in cyclonic combustion chamber at 1400 °C
P4.1*	In-line process for MSW	100% MSW	Pre-pyrolysis of MSW at 900 °C, then melting in combustion chamber at 1400 °C then electroreduction
P4.2	In-line process for MSW	100% MSW	Pre-pyrolysis of MSW at 900 °C, then melting in combustion chamber at 1400 °C then electroreduction
P5	Post-process for BA	100% BA	Three-phase combustion of BA in segmented oven (combustion, electroreduction, separation by gravity)
P6*	Post-process for BA	100% BA	Combustion of BA at 900 °C in fluidised bed under highly acidic conditions
P7	Post-process for BA	100% BA	Combustion of BA in rotating electric arc melting chamber
P8	Post-process for BA + FA	90% BA 10% FA	Not available
P9.1	Post-process for BA (fine fraction) + FA	80% BA_{fine} 20% FA	Pre-sieving of BA and mixing with FA, then combustion in electric arc melting chamber at 1400–1500 °C
P9.2	Post-process for BA (fine fraction) + FA	90% BA_{fine} 10% FA	Pre-sieving of BA and mixing with FA, then combustion in electric arc melting chamber at 1400–1500 °C
P10	Post-process for FA	100% FA	Direct combustion and melting of FA in plasma torch at 1350–1450 °C
P11*	Post-process for FA	100% FA	Combustion of FA at 900 °C in fluidised bed under highly acidic conditions
P12.1	Post-process for FA	100% FA (granulated form)	Combustion of FA in electric arc melting chamber at 1400–1500 °C
P12.2*	Post-process for FA	100% FA (granulated form)	Combustion of FA in electric arc melting chamber at 1400–1500 °C
P12.3*	Post-process for FA	100% FA (foamed form)	Combustion of FA in electric arc melting chamber at 1400–1500 °C
P13	Post-process for FA	100% FA	Combustion of FA in electrically heated melting chamber at 1350 °C
P14	Post-process for FA + FC	80% BA 20% FC	Combustion of BA and FC in plasma-heated rotating oven at 1200–1600 °C
P15.1	Post-process for FA + sewage sludge	50% BA 50% sewage sludge	Pre-heating at 700 °C, then combustion of BA and sewage sludge in melting chamber at 1600 °C
P15.2	Post-process for FA + sewage sludge	50% BA 50% sewage sludge	Pre-heating at 700 °C, then combustion of BA and sewage sludge in melting chamber at 1600 °C
P16*	Post-process for FA + cement	80% BA 20% cement	Not available
P17	Post-process for FA + recycled glass	70% BA 30% recycled glass	Combustion of FA and recycled glass in electrically heated melting chamber at 1350 °C
P18	Post-process for FA + car shred	53% FA 47% car shred	Combustion of FA and pre-sorted car shred in cyclonic melting chamber at 2000 °C
SON68	Vitrification of nuclear HLW	Synthetic borosilicate glass	Combustion of nuclear HLW with glass-forming mixture in induction-heated melting chamber at 1100 °C
R2bis*	Post-process for FA	100% FA	Combustion of FA in electric arc melting chamber at 1450 °C
R3	Post-process for FA	100% FA	Combustion of FA in electric arc melting chamber at 1800 °C

Samples are classified according to their parent high-temperature treatment process. Samples and standards labeled with an asterisk (e.g., P2*) exhibit vitrocrystallinity (i.e., > 2% of crystalline forms). Samples labelled Pi.j (e.g., P4.1*, P4.2) originate from the same process but differ in the operating conditions of the process, or in variations of their input material. MSW = municipal solid wastes; BA = bottom ash; FA = fly ash; FC = filter cake.

was considered in this study as a guide to durability. The two other glasses, R2bis* and R3, are among the few thoroughly studied waste glasses described in the literature (Colombel, 1996; Colombel et al., 1997). R2bis* and R3 were produced in France from the melting of fly ash by the same high-temperature treatment process (electric arc), but operated under different conditions of temperature and quenching. R2bis* is vitrocrystalline, while R3 is vitreous, which makes them representative analogs of the 23 samples.

Samples and standards were characterised by a multimethodological approach combining physical, microscopic and chemical analyses, and corrosion tests. All analyses and corrosion tests were performed under identical conditions for all samples.

2.2. Physical, microscopic and chemical analyses

Procedural details for the determination of the physical, microscopic and chemical characteristics of samples and standards are given elsewhere (Perret et al., 2000).

The crystallinity (XRD) and specific surface area S_{spec} (BET) of samples and standards were determined on ground fractions (sieved to 100–125 μm) after careful ethanol washing to remove the fine particles. The microscopic features (morphology, inclusions, surface and matrix structure) and semi-quantitative chemical homogeneity and composition of ground samples and standards were determined by SEM (using secondary electrons and back-scattered electron), while mineral phases were identified by SEM-EDS.

The chemical composition of samples and standards was measured by ICP-AES, ICP-MS, GF-AAS, colorimetry and HPLC, after dissolution by alkaline fusion or HF digestion. Measurements were performed in duplicate and were cross-calibrated with internal and external standard solutions.

2.3. Leaching behaviour

The MCC-1 test (Bates et al., 1994; Ebert and Mazer, 1994) was originally designed to study the corrosion of HLW glasses (4 cm^2 polished glass cubes in 40 ml H_2O at 90 °C during 28 days; no stirring, batch mode). Its interest for the present study lies in the fact that a large number of results obtained on various glasses are given in the literature (Jantzen, 1988; Jantzen and Plodinec, 1984; Plodinec and Wicks, 1994; Sproull et al., 1994).

However, because of the intrinsic nature of several of the present samples and standards (granules or fragile blocks), it was not possible to prepare polished monoliths for all samples. A modified MCC-1 corrosion test, the "Strasbourg test", was thus developed for the purpose of this study. The operating conditions of the Strasbourg test are discussed in detail by Perret et al. (2000) and summarised below.

A known mass (50 mg) of ground sample is sealed in a Teflon vessel containing ultrapure water (100 ml) at 90 °C ± 1 °C in a closed oven, for 1 day (6 samples), 3 days (26 samples), and 10 days (15 samples; duplicate test), without stirring and in batch mode.

To compare the results to those obtained by means of the MCC-1 test, at least during the initial stage of leaching, the parameter $\Delta t \cdot S_{glass}/V_{leachant}$ (physical extent of corrosion over the duration of the experiment) was kept within the same order of magnitude. For the MCC-1 test, $\Delta t \cdot S_{glass}/V_{leachant} = 2.8$ d/cm. For the Strasbourg test, and taking into account an average $S_{spec} = 400$ cm^2/g, $\Delta t \cdot S_{glass}/V_{leachant} = 0.2$–2 d/cm (1–10 days). Under these conditions, both tests can be compared, provided that the mechanisms of dissolution are far from equilibrium.

During corrosion, $pH_{leachate}$ evolves freely and is measured at the end of the experiment after filtering at 90 °C and cooling to room temperature. pH was measured after cooling as temperature changed too quickly and variably after removal from the oven and filtering. The concentrations of elements in the filtered leachate (0.2 μm) were then analysed as mentioned above.

Assuming that element release during corrosion is a congruent process, i.e. all elements are extracted from the glass matrix at the same normalised rate, the normalised apparent dissolution rate r_{glass} of a sample can be related to the normalised apparent loss of Si ΔNL_{Si} according to Eq. (1):

$$r_{glass} = r_{Si} = \Delta NL_{Si}/\Delta t = \left(\Delta[Si]_{leachate} V_{leachant} \cdot m_{glass}\right)/m_{Si} \cdot S_{glass} \cdot \Delta t \quad \left(g/m^2 \cdot d\right) \tag{1}$$

ΔNL_{Si}: normalised apparent loss of Si in the leachate (g/m^2)
Δt: duration of the corrosion experiment (d)
$\Delta[Si]_{leachate}$: variation of Si concentration in the leachate (g/l)
$V_{leachant}$: volume of leachant (l)
m_{glass}: initial mass of sample (g)
m_{Si}: initial mass of Si in the sample (g)
S_{glass}: surface of sample exposed to leachant (m^2)

Here, normalisation of the dissolution rate refers to the proportion of Si in the glass (m_{Si}/m_{glass}) and to the surface of glass subjected to the volume of leaching solution ($S_{glass}/V_{leachant}$).

Formally, dissolution rates should be expressed over the increments of corrosion time, i.e. for $\Delta t = 0$–1, 1–3 and 3–10 days respectively. However, the corrosion tests were performed on a new sample for each duration, making it difficult to take into account inter-sample variabilities in the calculation of the rates; the dissolution rates are thus expressed over global durations of corrosion, i.e. for $\Delta t = 0$–1, 0–3 and 0–10 days respectively, and may consequently be overestimated.

2.4. Determination of ΔG_{hydr}

On the basis of the model of Paul and Newton, the compositions of samples and standards were converted into silicates ($CaSiO_3$, $MgSiO_3$, Na_2SiO_3, K_2SiO_3, $BaSiO_3$, $ZnSiO_3$, $ZrSiO_4$) and oxides (SiO_2, Al_2O_3, CaO, Fe_2O_3, MnO_2, TiO_2). For the standard SON68, B_2O_3, Li_2SiO_3, Cs_2O_3, Nd_2O_3, $SrSiO_3$, NiO, MoO_3, La_2O_3, Ce_2O_3 were also introduced into the conversion.

Then, the equilibrium constants $K_{hydr(i)}$ for the hydration of these constituents at 90 °C were calculated using the simplified Van't Hoff law [Eq. (2)], assuming that the variation in heat capacity ΔC_p between 25 °C (T_0) and 90 °C (T_1) is constant (Linard, 2000):

$$\ln\left({}^{T_1}K_{hydr(i)}\right) = \ln\left({}^{T_0}K_{hydr(i)}\right) + \left(\left(\Delta H^0 - \Delta C_p \cdot T_0\right)/R\right)\cdot(1/T_0 - 1/T_1) + \left(\Delta C_p/R\right)\cdot\ln(T/T_0) \quad (2)$$

The pH-dependent speciation of the constituents was taken into account between pH = 1 and 12 for the determination of $K_{hydr(i)}$. In addition, Fe(III) and Mn(IV) were considered to be the dominant redox species of Fe and Mn respectively, on the basis of the claimed oxic conditions of the melting processes, and taking into account the fact that only minor traces of sulphides were detected. The value of $\Delta G_{hydr(i)}$ for the hydration of each of the constituents at 90 °C was then ascertained using Eq. (3):

$$\Delta G_{hydr(i)} = -R\cdot T\cdot\ln\left(K_{hydr(i)}\right) \quad \text{(cal/mol)} \quad (3)$$

Finally, the overall free energy of hydration ΔG_{hydr} of samples and standards at 90 °C was calculated according to Eq. (4):

$$\Delta G_{hydr} = \Sigma X_{(i)}\cdot\Delta G_{hydr(i)} \quad \text{(cal/mol glass)} \quad (4)$$

The complete set of thermodynamic data used to estimate the free energy of hydration of samples and standards is given in Table 2. Table 2 also lists the average proportions of the relevant species in all samples and standards, their corresponding $\Delta G_{hydr(i)}$ values at pH = 9.5 (average of pH measurements after 3 days corrosion), and their average contribution to the overall free energy of hydration ($X_{(i)}\cdot\Delta G_{hydr(i)}$).

The values of $K_{hydr(i)}$ of most of the trace elements present in the samples are not tabulated in the literature, or subject to large variability. These trace elements were thus not introduced into the numerical model for the calculation of the overall free energy of hydration, except for the species of Ba, Zn and Zr (known $K_{hydr(i)}$; non-negligible concentrations of these elements in some samples), and, with the standard SON68, for the species of B, Li, Cs, Nd, Sr, Ni, Mo, La and Ce (known $K_{hydr(i)}$; non-negligible concentration of the sum of these elements in the standard). The error in the determination of ΔG_{hydr} due to the missing $\Delta G_{hydr(i)}$ values of most of the trace elements present in the samples was considered to be negligible, because their $X_{(i)}$ contribution to the overall free energy is small, except for Cr (up to 7500 ppm) and Cu (up to 2500 ppm) in some samples.

The refined model of Jantzen, Plodinec and Wicks is claimed to take into account the surface precipitation of secondary minerals in the calculation of the overall free energy of hydration. However, the model used to integrate these secondary minerals is not readily available in the literature; for this reason, the authors did not introduce secondary minerals in the calculation, and the original model of Paul and Newton was applied.

3. Results and discussion

3.1. Physico-chemical characteristics

Fig. 1 shows examples of the various morphologies and grain sizes (photography), surface textures (SEM, secondary electrons) and bulk structure (SEM, backscattered electrons) of the samples provided by the companies.

According to XRD measurements (not shown), the majority of samples and standards (15 samples out of 23; 2 standards out of 3) are vitreous, i.e., they contain less than ca. 2% of crystalline phases. The others contain non-significant amounts of crystalline compounds and were classified as vitrocrystalline.

The specific surface areas of the ground samples and standards reflect their differences in bulk morphologies: For most samples, S_{spec} = 293–466 cm^2/g (standard glasses: 383–474 cm^2/g), with the notable exception of 6 samples (P1, P2*, P3*, P4.1*, P6* and P11*; ca. 600–8200 cm^2/g).

Vitreous samples, except P1, exhibit a low specific surface area, which is also the case for two vitrocrystalline samples (P12.1*, P16*) and one standard (R2bis*). Samples P6* (prepared from BA) and P11* (prepared from FA), which are characterised by extremely high values of S_{spec}, originate from the same high-temperature treatment process, which produces porous granules with aggregated particles in the sub-millimeter range.

Microscopic examination reveals the presence of several crystalline phases in the vitrocrystalline samples: the most commonly identified phases are quartz, gehlenite/melilite, diopside, Cr-rich spinel, albite, plagioclase, pyroxene, portlandite, and in some samples metal oxides, alloys and traces of sulphides. These phases, which are either inherited from the input material or formed at process temperature or during quenching of the melt, also contribute to the high specific surface area of most vitrocrystalline samples.

The results indicate that there is no direct link between the physical or microscopic characteristics of

Table 2a
Species taken into account for the calculation of the free energy of hydration of the samples and standards

Species	$X_{(i)}$	Reactions	pK	$\Delta G_{hydr(i)}$ (kcal/mol)	$X_{(i)}\cdot\Delta G_{hydr(i)}$ (kcal/mol)
$CaSiO_3$	0.37±0.14	$CaSiO_3 + 2H^+ + H_2O \rightarrow Ca^{2+} + H_4SiO_4$	−8.98 (25 °C)	−16.02	−6.00 ±2.20
SiO_2	0.18±0.19	$SiO_2 + 2H_2O \rightarrow H_4SiO_4$	2.97	3.83	1.12
		$H_4SiO_4 \rightarrow H_3SiO_4^- + H^+$	8.97		±0.75
		$H_3SiO_4^- \rightarrow H_2SiO_4^{2-} + H^+$	10.7		
Al_2O_3	0.17±0.07	$1/2(Al_2O_3 + 5H_2O) \rightarrow Al(OH)_4^- + H^+$	11	2.56	0.43
		$Al(OH)_4^- + H^+ \rightarrow Al(OH)_3 + H_2O$	−6.66		±0.22
		$Al(OH)_4^- + 2H^+ \rightarrow Al(OH)_2^+ + 2H_2O$	−12		
		$Al(OH)_4^- + 3H^+ \rightarrow AlOH^{2+} + 3H_2O$	−14.3		
		$Al(OH)_4^- + 4H^+ \rightarrow Al^{3+} + 4H_2O$	−17.6		
CaO	0.14±0.11	$CaO + 2H^+ \rightarrow Ca^{2+} + 2H_2O$	−17.6	2.36	0.52 ±0.46
$MgSiO_3$	0.08±0.04	$MgSiO_3 + 2H^+ + H_2O \rightarrow Mg^{2+} + H_4SiO_4$	−7.04	−12.79	−1.12 ±0.44
Na_2SiO_3	0.05±0.03	$Na_2SiO_3 + 2H^+ + H_2O \rightarrow 2Na^+ + H_4SiO_4$	−17.7	−30.58	−1.59 ±0.88
Fe_2O_3	0.04±0.03	$1/2(Fe_2O_3 + 6H^+ + 2e^-) \rightarrow 1/2(Fe^{2+} + 3H_2O)$	−7.54	+9.41	+0.44
		$Fe^{2+} + OH^- \rightarrow FeOH^+$	−5.51		±0.35
		$Fe^{2+} + 2H_2O \rightarrow Fe(OH)_2 + 2H^+$	16.8		
		$Fe^{2+} + 3H_2O \rightarrow Fe(OH)_3^- + 3H^+$	25.3		
		$Fe^{2+} + 4H_2O \rightarrow Fe(OH)_4^{2-} + 4H^+$	45.1 (25 °C)		
		$Fe^{2+} + 3H_2O \rightarrow Fe(OH)_3 + 3H^+ + e^-$	25.5		
		$Fe^{2+} \rightarrow Fe^{3+} + e^-$	11.8		
		$Fe^{3+} + OH^- \rightarrow FeOH^{2+}$	−11.4		
		$Fe^{3+} + 4H_2O \rightarrow Fe(OH)_4^- + 4H^+ + e^-$	29.3		
K_2SiO_3	0.01±0.006	$K_2SiO_3 + 2H^+ + H_2O \rightarrow 2K^+ + H_4SiO_4$	−26.2	−44.6	−0.48 ±0.28
$ZnSiO_3$	0.007±0.01	$ZnSiO_3 + 3H_2O \rightarrow Zn(OH)_2 + H_4SiO_4$	−15.4	−26.88	−0.19 ±0.26
MnO_2	0.003±0.002	$MnO_2 + 2e^- + 4H^+ \rightarrow Mn^{2+} + 2H_2O$	20.4	+132.41	+0.35
		$Mn^{2+} + H_2O \rightarrow MnOH^+ + H^+$	8.79		±0.25
		$Mn^{2+} + 3H_2O \rightarrow Mn(OH)_3^- + 3H^+$	24.9		
		$Mn^{2+} + 4H_2O \rightarrow Mn(OH)_4^{2-} + 4H^+$	48.3 (25 °C)		
		$Mn^{2+} + 1/2H_2O \rightarrow 1/2Mn_2OH^{3+} + 1/2H^+$	5.3 (25 °C)		
		$Mn^{2+} + 3/2H_2O \rightarrow 1/2Mn_2(OH)_3^+ + 3/2H^+$	11.9 (25 °C)		
$ZrSiO_4$	0.002±0.004	$ZrSiO_4 + 2H^+ + H_2O \rightarrow Zr^{4+} + H_4SiO_4$	12 (25 °C)	−28.65	−0.05 ±0.11
$BaSiO_3$	0.002±0.002	$BaSiO_3 + 2H^+ + H_2O \rightarrow Ba^{2+} + H_4SiO_4$	−19.4	−27.36	−0.06 ±0.46

Species are listed in the order of their decreasing concentration in waste glasses. The reactions of hydration and H^+ or e^- exchange are given for each species, with their corresponding pK at 90 °C, except where otherwise stated (adapted from Advocat, 1991, and references therein). The reactions of H_4SiO_4 produced during the hydrolysis of the various silicates are taken into account and mentioned under the species SiO_2. $X_{(i)}$ denotes the average molar fractions of species in all samples and standards (individual values of $X_{(i)}$ may vary by a factor of up to 2 from sample to sample). $\Delta G_{hydr(i)}$ is the corresponding free energy of hydration of the species, calculated for pH = 9.5 (average of pH measurements after 3 days). $X_{(i)}\cdot\Delta G_{hydr(i)}$ represents the average contributions of the species in all samples and standards, at the pH measured individually after 1 day, 3 days, 10 days.

Table 2b
Additional species taken into account for the calculation of the free energy of hydration of the standard SON68

Species	$X_{(i)}$	Reactions	pK	$\Delta G_{hydr(i)}$ (kcal/mol)	$X_{(i)}\cdot\Delta G_{hydr(i)}$ (kcal/mol)
B_2O_3	0.187	$1/2(B_2O_3+3H_2O) \rightarrow B(OH)_3$ $B(OH)_3 \rightarrow H_2BO_3^- + H^+$ $H_2BO_3^- \rightarrow HBO_3^{2-} + H^+$	−3.12 8.56 (25 °C) 12.7 (25 °C)	−6.83	−1.12 ±0.04
Li_2SiO_3	0.061	$Li_2SiO_3 + 2H_2O \rightarrow 2Li^+ + H_4SiO_4$	−13.8	−24.02	−1.42 ±0.007
MoO_3	0.011	$MoO_3 + H_2O \rightarrow MoO_4^{2-} + 2H^+$ $MoO_4^{2-} + H^+ \rightarrow HMoO_4^-$ $MoO_4^{2-} + 2H^+ \rightarrow H_2MoO_4$	11.1 −4.24 (25 °C) −7.94	−13.14	−0.12 ±0.009
$Nd_2O_3 + Cs_2O_3$	0.008	$1/2(Nd_2O_3 + 6H^+) \rightarrow Nd^{3+} + 3/2H_2O$ $Nd^{3+} + H_2O \rightarrow NdOH^{2+} + H^+$ $Nd^{3+} + 4H_2O \rightarrow Nd(OH)_4^- + 4H^+$ $Nd^{3+} + H_2O \rightarrow 1/2Nd_2(OH)_2^{4+} + H^+$	−22.5 7.99 (25 °C) 37.4 (25 °C) 6.94 (25 °C)	+6.10	+0.03 ±0.006
NiO	0.006	$NiO + H_2O \rightarrow Ni(OH)_2$ $Ni(OH)_2 + 2H^+ \rightarrow Ni^{2+} + 2H_2O$ $Ni(OH)_2 + H^+ \rightarrow NiOH^+ + H_2O$ $Ni(OH)_2 + H_2O \rightarrow Ni(OH)_3^- + H^+$	6.53 (25 °C) −19.0 (25 °C) −9.34 (25 °C) 11.0 (25 °C)	+10.14	+0.05 ±0.004
$La_2O_3 + Ce_2O_3$	0.005	$1/2(Ce_2O_3 + 6H^+) \rightarrow Ce^{3+} + 3/2H_2O$ $Ce^{3+} + H_2O \rightarrow CeOH^{2+} + H^+$ $Ce^{3+} + H_2O \rightarrow 1/2Ce_2(OH)_2^{4+} + H^+$ $Ce^{3+} + H_2O \rightarrow Ce(OH)^{3+} + H^+ + e^-$ $Ce^{3+} + 2H_2O \rightarrow Ce(OH)_2^{2+} + 2H^+ + e^-$	−30.4 (25 °C) 8.3 (25 °C) 7.75 (25 °C) 28.4 (25 °C) 29.2 (25 °C)	−5.27	−0.04 ±0.005
$SrSiO_3$	0.003	$SrSiO_3 + 2H^+ + H_2O \rightarrow Sr^{2+} + H_4SiO_4$	−14.9	−25.90	−0.08 ±0.0003

This glass is treated separately, as it contains non-negligible proportions of species not present in the other waste glasses. The coefficients of variation given for $X_{(i)}\cdot\Delta G_{hydr(i)}$ are much smaller than in Table 2a, because $X_{(i)}$ is constant for SON68, and because $\Delta G_{hydr(i)}$ varies only over a very narrow range for the pH values measured at the end of the corrosion experiments of SON68 ($pH_{3\ days} = 8.63$; $pH_{10\ days} = 8.98$).

the samples and standards, and the process from which they are produced (i.e., in-line processes or post-processes) or the input material (i.e., MSW, BA, FA, FC, additives) used to produce them. Fig. 2 shows the content of major, minor and trace species in the samples and standards, as determined by bulk chemical analyses.

It is well established that SiO_2 (Si: network-forming element) is the most important key parameter for defining durable glasses (Grambow, 1985; Paul, 1982; Grambow and Strachan, 1983; Vernaz et al., 1990; Crovisier et al., 1987, 1992a). In the present samples, the average $[SiO_2]$ content is 41.4±8.4%.

Al_2O_3, with Al, either a network-forming element (tetrahedral position in the glass matrix) or a network-modifying element (octrahedral position, when combined with Na or K), is apparently influencing the durability of glasses in the same manner as SiO_2 (Paul, 1982; Scholze, 1991). In the samples, the average $[Al_2O_3]$ content is 16.6±6%.

For all samples and standards, ($[SiO_2]+[Al_2O_3]$) ranges between 45 and 75%. The studied waste glasses are thus expected to be stable, provided that they have a dominantly vitreous nature.

Calcium, on the other hand, is known to act as a network-modifying element and may have a detrimental effect on glass durability when it is present in high proportions (e.g., >15% CaO; Scholze, 1991). In the samples, the average [CaO] content is 23.1±8.1%.

In the case of the present samples, the proportions of the major constituents do not necessarily have an influence on the proportion of crystalline material, and they are not distinctly affected by the type of high-temperature treatment process from which they originate.

However, post-processes treating fly ash (or FA in combination with other additives) exhibit on average a lower [SiO_2]:[CaO] ratio (average = 1.4; range = 0.8–2.6) than in-line processes (average = 2.9; range = 0.8–5.1) or post-processes treating bottom ash (or BA in combination with other additives; average = 2.9; range = 1.9–4). This is explained by the fact that Si-rich components are poorly volatile, leaving fly ashes resulting from the incineration of municipal solid wastes depleted in SiO_2.

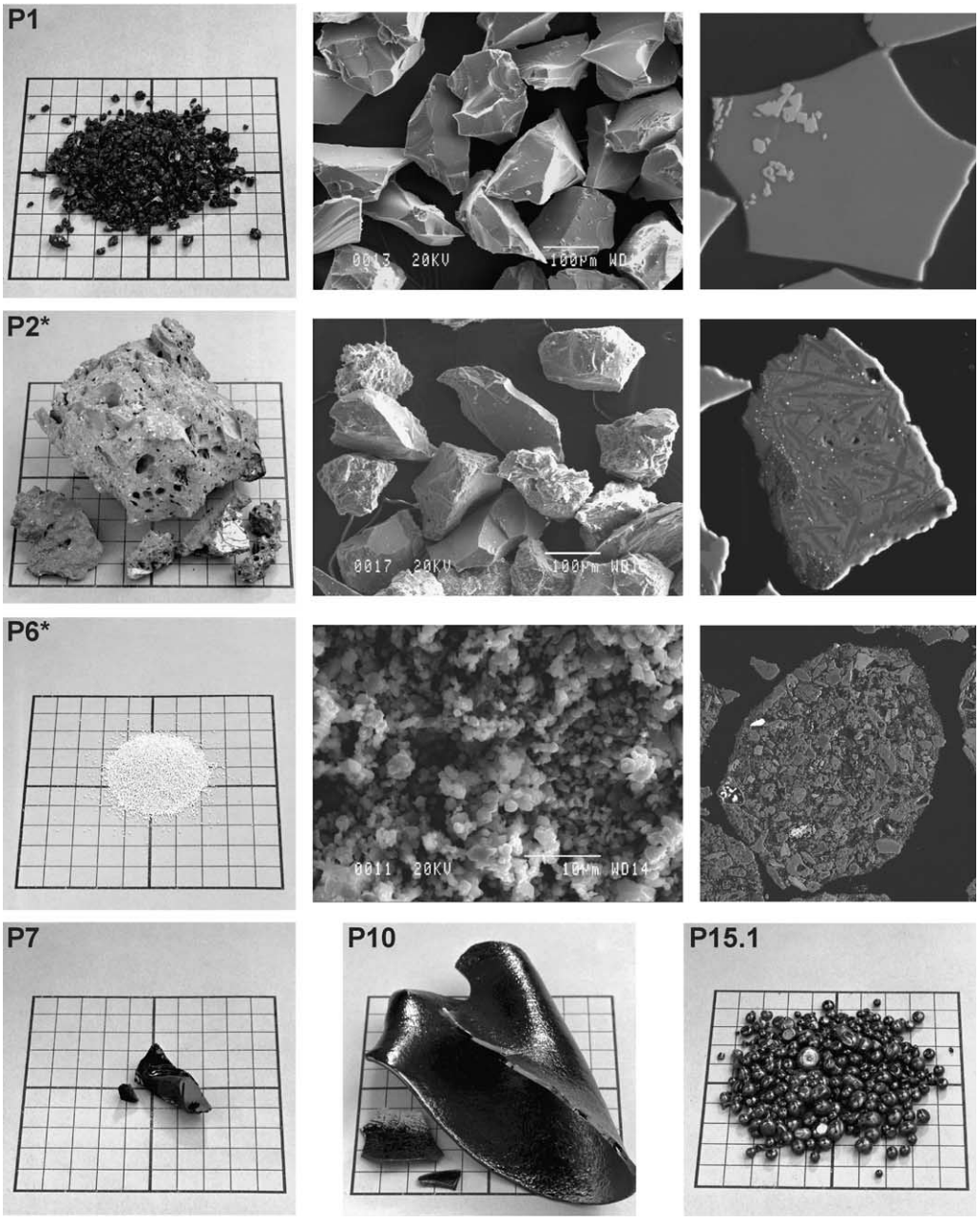

Fig. 1. Typical morphologies and sizes of the waste samples. First row: vitreous sample P1 (conventional photograph; SEM-SE; SEM-BSE, base length = 145 μm). Second row: vitrocrystalline sample P2* (conventional photograph; SEM-SE; SEM-BSE, base length = 178 μm). Third row: vitrocrystalline sample P6* (conventional photograph; SEM-SE; SEM-BSE, base length = 772 μm). Fourth row: vitreous samples P7, P10 and P15.1 (conventional photographs). Conventional photographs are taken from samples as provided, over a 10×10 cm grid background. SEM-SE micrographs are taken from ground samples (100–125 μm). SEM-BSE micrographs are taken from ground samples embedded in epoxy resin and post-polished.

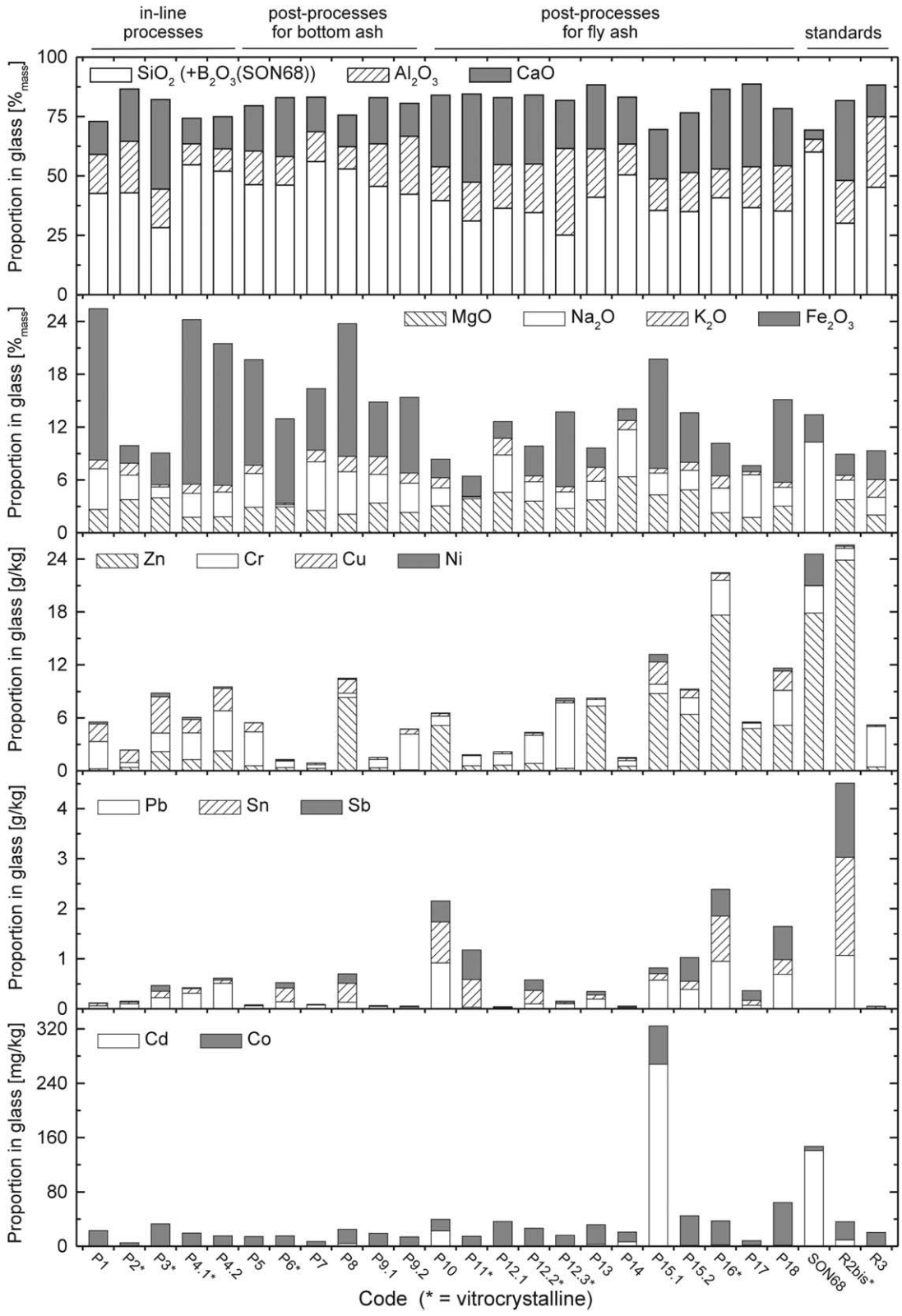

Fig. 2. Proportions of major, minor and trace elements in samples and standards, as determined from chemical analyses.

3.2. Leaching behaviour

The complete description of the behaviour of samples and standards during corrosion is detailed elsewhere (Perret et al., 2000), and only the most striking trends are discussed below.

Samples and standards were corroded according to the Strasbourg test, designed for the purpose of the present study and derived from the MCC-1 test. The concentrations of the major elements Si, Al and Ca measured in the filtered leachates at the end of the corrosion experiments are shown in Fig. 3.

The temporal evolution of major elements in the leachates gives clues to the mechanisms and apparent matrix dissolution rates of the glasses. Information on the absolute dissolution rate, i.e., the rate at which elements are extracted from the glass network, is obscured by the fact that during corrosion, significant proportions of many released elements are immobilised into secondary minerals or precipitated at the solid-solution interface, and also because most glasses are observed to develop a gel layer which partly scavenges the extracted elements and may inhibit reaction progress (Malow, 1982; Crovisier et al., 1987, 1992b; Petit et al., 1990; Vernaz and Dussossoy, 1992; Grambow, 1994).

On the basis of the 1-day corrosion experiment, $[Si]_{leachate}$ ranges from 0.3 mg/l (P4.1*) to 6.3 mg/l (P12.2*), while $[Al]_{leachate}$ ranges from 0.07 mg/l (P4.1*) to 5.6 mg/l (P12.3*), and $[Ca]_{leachate}$ ranges from 0.3 mg/l (P4.1*) to 8.6 mg/l (P3*). Generally, the sample-to-sample fingerprints of $[Si]_{leachate}$, $[Al]_{leachate}$ and $[Ca]_{leachate}$ are dissimilar.

$[Na]_{leachate}$ (0.02–1.3 mg/l after 1 day, 0.5–2.6 mg/l after 3 days) and $[K]_{leachate}$ (0.07–1.0 mg/l after 1 day, 0.08–1.1 mg/l after 3 days) are fairly low, but these elements show amongst the highest release propensity, as depicted in Table 3 for 3 days corrosion: $\{[Na]_{leachate}$ [mg/l]$\}:\{[Na]_{glass}$ [g/g]$\} = 4$–172 after 1 day, 26–375 after 3 days; $\{[K]_{leachate}$ [mg/l]$\}:\{[K]_{glass}$ [g/g]$\} = 5$-184 after 1 day, 14–381 after 3 days. This indicates that Na and K are not scavenged into secondary minerals, or to a much lower extent than Si, Al, Ca, or Mg (for these 4 elements, $[conc]_{leachate}:[conc]_{glass} \approx 1$–55 after 1 day, 5–65 after 3 days). On the basis of the results, it is however

Table 3
Degree of congruency of the releases determined on a set of major, minor and trace elements after 3 days corrosion. Data are rounded to the nearest figure

	$\{[conc]_{leachate}\}:\{[conc]_{glass}\}$ (mg/l):(g/g)											
Sample	Si	Al	Ca	Mg	Na	K	Fe	Mn	Sr	Zn	Zr	Pb
P1	36	41	46	40	50	32	0.2	0.6	46	195	0.2	5
P2*	36	35	50	22	62	69	0.9	1.4	51	82	0.9	9
P3*	50	55	51	11	128	184	–	–	78	–	0.2	2
P4.1*	5	6	7	11	31	23	–	–	12	16	–	–
P4.2	23	30	29	32	38	32	0.1	–	38	7	–	1
P5	35	39	40	34	56	55	2.7	1.0	42	124	0.1	8
P6*	16	22	37	8	258	65	0.1	1.3	59	268	0.1	3
P7	17	19	21	18	27	24	0.4	2.5	21	78	0.6	7
P8	24	26	27	23	37	22	1.2	1.7	26	8	0.9	16
P9.1	35	39	43	38	64	37	0.3	1.6	48	322	0.3	5
P9.2	29	30	31	35	48	55	–	4.1	34	81	–	2
P10	47	51	45	23	83	60	–	–	60	2	–	0.1
P11*	24	45	45	17	375	381	0.4	–	63	94	–	14
P12.1	52	52	64	9	79	68	–	–	74	41	0.3	12
P12.2*	48	50	50	16	86	75	–	–	69	43	–	1
P12.3*	56	47	57	17	87	94	–	–	62	–	0.3	1
P13	45	48	51	28	79	37	0.3	–	60	7	<0.1	1
P14	32	37	37	36	41	55	3.1	4.2	47	37	<0.1	9
P15.1	39	44	38	42	63	58	0.2	0.5	42	2	<0.1	0.3
P15.2	42	48	44	36	64	31	0.3	1.0	49	6	<0.1	0.6
P16*	47	49	49	17	65	36	–	–	57	1	0.8	0.3
P17	62	65	58	25	73	152	–	–	76	3	–	2
P18	41	50	47	34	72	56	–	–	55	1	–	<0.1
SON68	21	21	35	–	26	–	0.1	1.1	24	2	–	12
R2bis*	43	44	43	21	83	104	1.5	2.7	60	3	0.1	1
R3	17	16	19	23	42	14	–	–	20	–	<0.1	6
Average	36	39	41	25	81	73	0.7	1.8	49	62	0.3	5
std.dev.	14	14	13	10	75	76	0.9	1.2	18	89	0.3	5

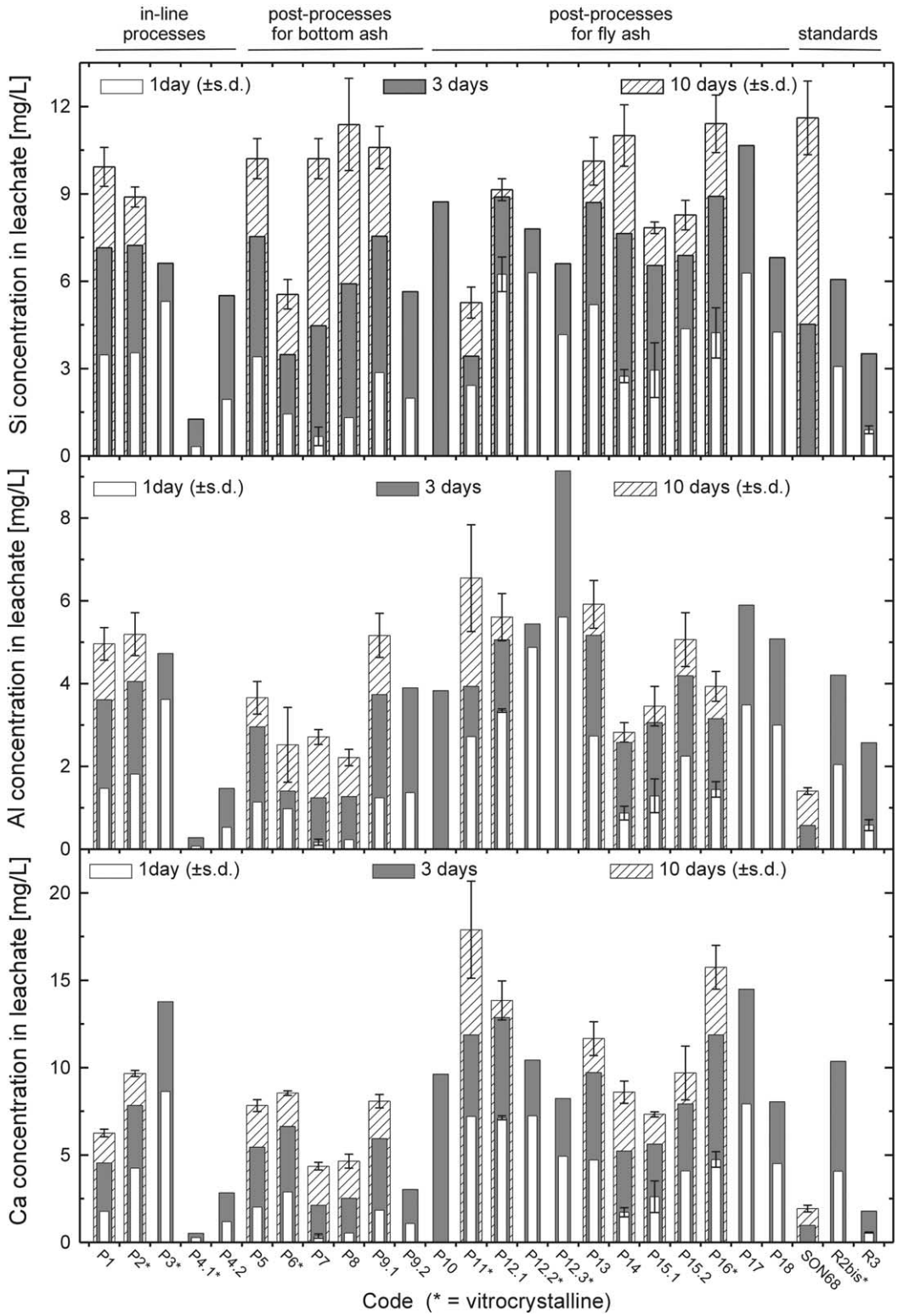

Fig. 3. Evolution of the apparent releases of Si, Al and Ca in the leachates of the Strasbourg corrosion test after 1, 3 and 10 days. The minimum and maximum concentrations are indicated for experiments that were performed in duplicate.

not possible to indicate if the alkali elements Na and K are extracted from the glass matrix by an ion-exchange mechanism, as is often the case for, e.g. soda-lime glasses (Scholze, 1991). The evolution of the pH (7.0–10.2 after 1 day, 8.3–10.3 after 3 days) is discussed below.

The element-to-element and sample-to-sample differences are great for the releases of minor and trace elements (see Table 3), with several elements exhibiting a contrasting behaviour (e.g., $\{[Zn]_{leachate}\}:\{[Zn]_{glass}\}\approx 1$-268 after 3 days). However, Table 4 shows that the maximum concentrations of trace elements are systematically very low, whatever the duration of the corrosion experiment: $[M]_{leachate} < 0.01$–5 μg/l for Co, Cd, Sn, Pb, and $[M]_{leachate} < 10$–100 μg/l for Cr, Ni, Cu, Zn, Sb.

As indicated in Table 4, the leachates of the waste glasses fulfill the requirements of the Swiss guidelines for the disposal of waste residues in landfills for inert materials (TOW: Technical Ordinance on Wastes), although the TOW leaching test (designed for the assessment of bottom ash and fly ash) is performed under less aggressive conditions than the Strasbourg test. In addition, the concentrations of trace metals released during the corrosion test are much lower than the maximum allowed concentrations which can be released by industries (MSW incineration plants or other industrial activities) in natural waters, as stated by the Swiss Ordinance for the Protection of Waters (OPW). This is an important observation that the waste glasses not only embed large amounts of trace metals, but also retain them during corrosion, either in the vitreous matrix, or scavenged in the secondary minerals. However, no trend was observed between the corrosion

Table 4
Concentrations of heavy metals measured in the leachates of the Strasbourg test

Sample	Cr (μg/l)	Co (μg/l)	Ni (μg/l)	Cu (μg/l)	Zn (μg/l)	Cd (μg/l)	Sn (μg/l)	Pb (μg/l)
P1	29	0.05	11	14	45	0.4	0.1	0.3
P2*	28	0.04	10	17	32	0.6	0.2	0.9
P3*	<5	0.04	<5	<5	2	0.01	0.2	0.5
P4.1*	<5	0.04	<5	<5	21	0.03	0.03	0.01
P4.2	<5	0.02	<5	<5	15	0.03	0.08	0.4
P5	34	0.05	19	16	71	2.7	0.2	0.5
P6*	26	0.03	13	13	98	0.6	0.1	0.4
P7	28	0.2	12	15	47	0.3	0.2	0.5
P8	32	0.2	14	19	68	0.9	0.6	2.5
P9.1	30	0.03	14	13	113	0.9	0.1	0.3
P9.2	<5	0.01	<5	<5	10	<0.02	0.1	0.07
P10	<5	0.03	<5	<5	9	0.03	0.5	0.1
P11*	26	0.06	<10	10	54	0.7	0.2	0.4
P12.1	40	0.1	12	16	26	1.7	0.1	0.2
P12.2*	<5	0.08	<5	<5	36	0.05	0.3	0.1
P12.3*	<5	0.1	<5	<5	2	0.1	0.2	0.1
P13	30	0.05	<5	11	52	1.5	0.2	0.3
P14	30	0.06	<5	12	19	0.4	0.1	0.3
P15.1	26	0.2	<5	14	19	0.4	0.1	0.2
P15.2	28	0.04	12	13	36	2	0.3	0.2
P16*	36	0.4	22	15	37	2.3	0.7	0.7
P17	<5	0.03	<5	<5	40	0.05	0.6	0.2
P18	<5	0.02	<5	<5	8	0.01	0.3	0.07
SON68	68	<10	13	11	42	1.1	0.05	0.1
R2bis*	<5	0.04	<5	<5	143	<0.01	3.6	2.1
R3	<5	0.2	<5	<5	9	0.06	0.1	0.08
TOW	50	–	200	200	1000	10	–	100
OPW (MSW)	100	–	100	100	100	50	–	100
OPW (non-MSW)	2000	–	2000	500	2000	100	–	500

For each sample and standard, the highest concentrations measured after 1 or 3 or 10 days corrosion is given. For each element, the maximum concentration measured of all samples and standards is underlined. For comparison, some Swiss guidelines are given. The row "TOW" indicates the maximum allowed concentrations of metals in the leachate of the corrosion test performed under the conditions of the Swiss Technical Ordinance on Wastes (TOW; TVA/OTD), which states the limits under which a waste material can be disposed off in landfills for inert material (SAEFL, 1996). The row "OPW (MSW)" indicates the maximum allowed concentrations of metals which can be released in natural waters by MSW incineration plants (Swiss Ordinance for the Protection of Waters; SAEFL, 1998). The row "OPW (non-MSW)" indicates the maximum allowed concentrations of metals which can be released in natural waters by industrial effluents.

behaviour of waste glasses and their release of trace elements.

The results clearly indicate that the apparent matrix dissolution process follows different pathways from sample to sample and from element to element. This highlights the complex solution and secondary phase chemistries involved during corrosion, and confirms that the dissolution of domestic waste glasses does not follow a simple congruent mechanism of release (Grambow, 1985; Advocat, 1991).

This behaviour cannot be explained in terms of process categories (in-line processes; post-processes) or crystallinity of the waste glasses studied, and hampers a clear assessment of the long-term stability of these materials on the exclusive basis of their release during accelerated batch corrosion tests.

Among possible mechanisms explaining the observations, SEM measurements of samples after corrosion (see Perret et al., 2000) indicate that trace elements extracted out of the silicate network are frequently scavenged by the secondary products which develop at the surface of glasses during corrosion. This behaviour must be considered as a favourable characteristic of the studied waste glasses with respect to the immobilisation of toxic elements. Scavenging of heavy metals by the gel layer is very probable but requires more sophisticated microscopic techniques to be demonstrated (Malow, 1982; Ehret et al., 1986; Petit et al., 1990; Crovisier et al., 1992b; Vernaz and Dussossoy, 1992).

The following secondary mineral phases have been observed at the surfaces of the samples and standards: Ca-rich phases (e.g., Ca–P, Ca–P–Ti, Ca–Fe–Ti), Si-rich phases and coatings (e.g., zeolites, Si–P, Ca-silicates, Si–Al–Mg(–Ca), Si–Al–Ca–Fe).

3.3. Free energy of hydration

The evolution of the free energies of hydration of the samples and standards as a function of pH, calculated on the basis of the chemical composition of the provided materials, is given in Fig. 4 for the different categories of processes and for the 3 standards. The range of pH values measured at the end of the 1-, 3- and 10-day corrosion experiments (pH = 7.0–10.3) is indicated as a shaded area on the figures.

As the model of Paul and Newton is formally designed for vitreous materials with an homogeneous silicate network, the results obtained on the vitrocrystalline materials may be questioned; they are however shown (dotted lines in Fig. 4) for comparative purposes, assuming that their crystallinity is not large enough to impair significantly the overall free energy of hydration.

These calculations show at a first glance that, taken collectively, the thermodynamic stability of waste glasses towards hydration is at a maximum around pH = 5–7.5. As expected from theoretical considerations and experimental observations (e.g., Paul, 1982), glass hydration becomes more spontaneous under alkaline conditions (pH > 10) than under acidic conditions (pH < 4).

The observed sample-to-sample variability in ΔG_{hydr} values is fairly large. Considering the pH values measured at the end of the corrosion experiments, ΔG_{hydr} ranges from +0.1 kcal/mol (P4.1*; pH = 7.9 after 1 day; thermodynamically most stable sample) to −12.6 kcal/mol (P10; pH = 9.9 after 3 days; least stable sample). Nevertheless, the studied waste glasses display stabilities comparable to that of the French nuclear HLW glass SON68 (ΔG_{hydr}(SON68) = −7.0 kcal/mol; pH = 9.0 after 10 days), which is a positive indication for the long-term stability of the waste glasses.

The time-averaged value (1, 3, 10 days) of ΔG_{hydr} for the samples produced by post-processes for FA (−9.6 kcal/mol ± 2.0) is more negative than for the samples produced by in-line processes (−4.7 kcal/mol ± 3.1) or post-processes for BA (−5.0 kcal/mol ± 1.5). This in turn indicates that post-processes for FA produce materials with a lower thermodynamic stability, suggesting that the $[SiO_2]_{glass}$:$[CaO]_{glass}$ ratio plays a major role in the thermodynamic behaviour of waste glasses.

Additionally, the $[SiO_2]_{glass}$:$[CaO]_{glass}$ ratio influences the shape of the pH profiles of ΔG_{hydr} (Fig. 4). This is clearly illustrated in samples with a low $[SiO_2]_{glass}$:$[CaO]_{glass}$ ratio, which show a steeper slope in the acidic region (e.g., P3*, P11*, P17), while samples with a high $[SiO_2]_{glass}$:$[CaO]_{glass}$ ratio show a steeper slope in the alkaline region (e.g., P4.1*, P8, SON68).

Indeed, for a given sample composition, the overall free energy of hydration is primarily controlled by those species showing large $\Delta G_{hydr(i)}$ values and being present in major proportions (see Table 2).

For all samples, the most important contribution to the overall free energy of hydration is given by the component $CaSiO_3$ ($X_{(i)}$ = 17–63 mol%; $\Delta G_{hydr(i)}$ = −16 kcal/mol), which strongly reduces the thermodynamic stability of waste glasses. Although their sum represents only 8–19 mol% of the average waste glass composition, Na_2SiO_3 ($X_{(i)}$ = 0.3–9 mol%; $\Delta G_{hydr(i)}$ = −30.6 kcal/mol) and $MgSiO_3$ ($X_{(i)}$ = 4–16 mol%; $\Delta G_{hydr(i)}$ = −12.8 kcal/mol) also reduce glass stability, but to a lesser extent.

The stabilising influence of the components SiO_2, Al_2O_3, CaO, Fe_2O_3, and even MnO_2 on the overall stability of waste glasses is weak in comparison to the destabilising effect of most silicate polyhedra (see Table 2). Finally, the effect of heavy metals on the thermodynamic stability of glasses can be neglected due to their low proportions in waste glasses (< 1 mol%). Indeed, heavy metals or other elements may chemically stabilise waste glasses during corrosion, favouring the nucleation of secondary products or leading to hydroxides which will inhibit further corrosion (Paul, 1982; Scholze, 1991); nevertheless, these effects are not taken

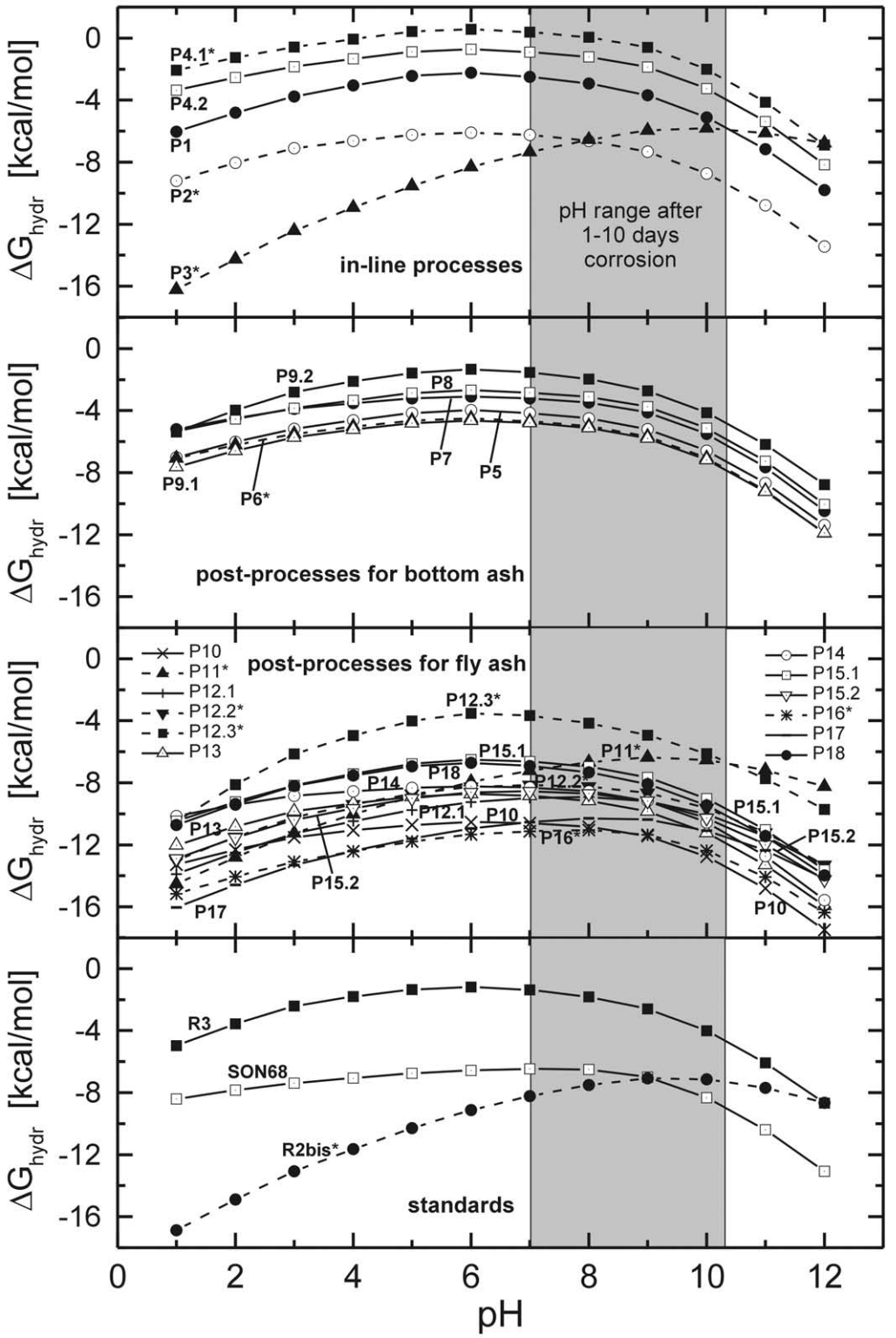

Fig. 4. Evolution of the calculated free energy of hydration of samples and standards as a function of the pH of the leachate. Formally, the model applies exclusively to vitreous materials (solid curves); vitrocrystalline samples are shown with dashed curves. The shaded area represents the range of pH values measured at the end of the 1-, 3- and 10-day corrosion experiments.

into account in the thermodynamic model, which considers that the hydrolysis of the glass network is the driving force behind its dissolution.

The results indicate that glasses containing large proportions of network-forming elements (primarily Si and Al) and the weakest possible proportions of network-modifying elements (primarily Ca, Na, Mg and K) will exhibit the highest thermodynamic stabilities. Data in Table 2 also suggest that a fine tuning of the proportion of Mn in waste glasses would strongly influence their overall stability: For instance, 1 mol% MnO_2 would already contribute +1.3 kcal/mol of the overall free energy, counteracting the destabilising influence of, e.g., 8 mol% $MgSiO_3$. In addition, it is expected that leached Mn would precipitate as hydroxides at the surface of glasses, acting as a powerful metal scavenger during corrosion.

The calculated thermodynamic stabilities of waste glasses are in agreement with the observed leaching behaviour from the literature, that show lower stability at higher pH (Schloze, 1991). Indeed, the pH of the leachate, which evolves freely during the Strasbourg corrosion test, is a direct consequence of the relative proportion of Ca in waste glasses. Fig. 5 shows the strong relationships existing between $pH_{leachate}$, $[Ca]_{leachate}$ and $[Ca]_{glass}$ on one hand, and also between ΔG_{hydr}, $[Ca]_{glass}$ and $pH_{leachate}$.

After 3 days corrosion, the relationships $[Ca]_{leachate}$ vs. $[Ca]_{glass}$ ($r=0.949$) and $pH_{leachate}$ vs. $[Ca]_{glass}$ ($r=0.887$) are fairly tight, indicating that pH is governed mostly, but not exclusively, by the dissolution of Ca species. The effect of their dissolution on the evolution of alkaline conditions is given by reactions 3 and 4:

$$\{CaO\}_{glass}+2H_2O \rightarrow Ca^{2+}+2OH^- \quad \text{(reaction 3)}$$

$$\{CaSiO_3\}_{glass}+2H_2O \rightarrow Ca^{2+}+H_4SiO_4+2OH^- \quad \text{(reaction 4)}$$

The influence of Ca on $pH_{leachate}$ is weaker for Ca-poor samples, and also after only 1 day corrosion (not shown); this is because the initial evolution of the pH is preferentially driven by the dissolution of the Na-rich and K-rich alkaline species.

As already mentioned, the overall free energy of hydration is mainly, but not exclusively, governed by the presence of Ca in waste glasses; this helps to explain the relative scatter of data in the plot of ΔG_{hydr} vs. $[Ca]_{glass}$ or $pH_{leachate}$.

It is remarkable to notice that the correlations of Fig. 5 are good, though each sample and standard originates from a different high-temperature treatment process operated on different categories of input material (MSW; BA, FA, FC or combinations of them with possible additives). In that respect, it is concluded that the free energy of hydration of waste glass can be explained in terms of few parameters, namely the content of Ca in glasses and the pH of the leachate resulting primarily from dissolution of Ca species during leaching by water.

Under certain circumstances, Na and K are expected to reduce the stability of glasses by favouring the formation of phase-separated glasses with reduced resistance to corrosion (Sholze, 1991). In the present samples, ($[Na_2O]+[K_2O]$) ranges between 0.3 and 6.8% (up to 10.3% for the standard SON68); the effect of these species on the thermodynamic and chemical durability of the samples is thus expected to be minor.

The estimation of the free energy of hydration of waste glasses is a convenient numerical approach, requiring only the determination of the chemical composition of the samples.

3.4. Chemical leaching vs thermodynamic stability

A way of validating the ΔG_{hydr} approach for the waste glasses is given in Fig. 6, which shows the relationship existing between the normalised apparent dissolution rate of glass r_{glass}, and ΔG_{hydr} for the corrosion experiments performed during 1, 3 and 10 days. For comparison, the curves of Fig. 6d (data from the literature) are reproduced in Fig. 6a–c. These curves, labelled "MCC-1 test", show the relationship between the calculated free energy of hydration of 115 glasses of different origins (nuclear HLW glasses; commercial, medieval, antique and natural glasses) and their normalised release rate during the typical MCC-1 corrosion test applied for the assessment of the performances of nuclear HLW glasses in the USA (Plodinec and Wicks, 1994).

The apparent dissolution rates of glasses r_{glass} are calculated from the apparent release rates of Si in the leachates, and expressed as normalised rates [see Eq. (1)] to compensate the differences in specific surface areas ($S_{spec}=293$-8197 cm^2/g) between samples, their broad Si content ($[SiO_2]_{glass}=25$–56 mass%), and the duration of the corrosion tests ($\Delta t=1$–10 days).

Indeed, it has been shown that Si precipitates into secondary minerals at the surface of glasses during corrosion (see, e.g., Fig. 1), and the choice of this element for the assessment of r_{glass} may be questioned. However, Si is the most abundant element in the composition of the waste glasses, and its degree of congruency after 3 days corrosion (36 ± 14, see Table 3), though not as high as for Na (81 ± 75) and K (73 ± 76), is large enough and among the least variables to consider Si as the most appropriate indicator of apparent matrix dissolution.

With the exception of samples P2*, P6* and P11*, which present excessively high specific surface areas (ca. 10–20× larger than most other samples and standards) and thus artificially bias the calculation of the

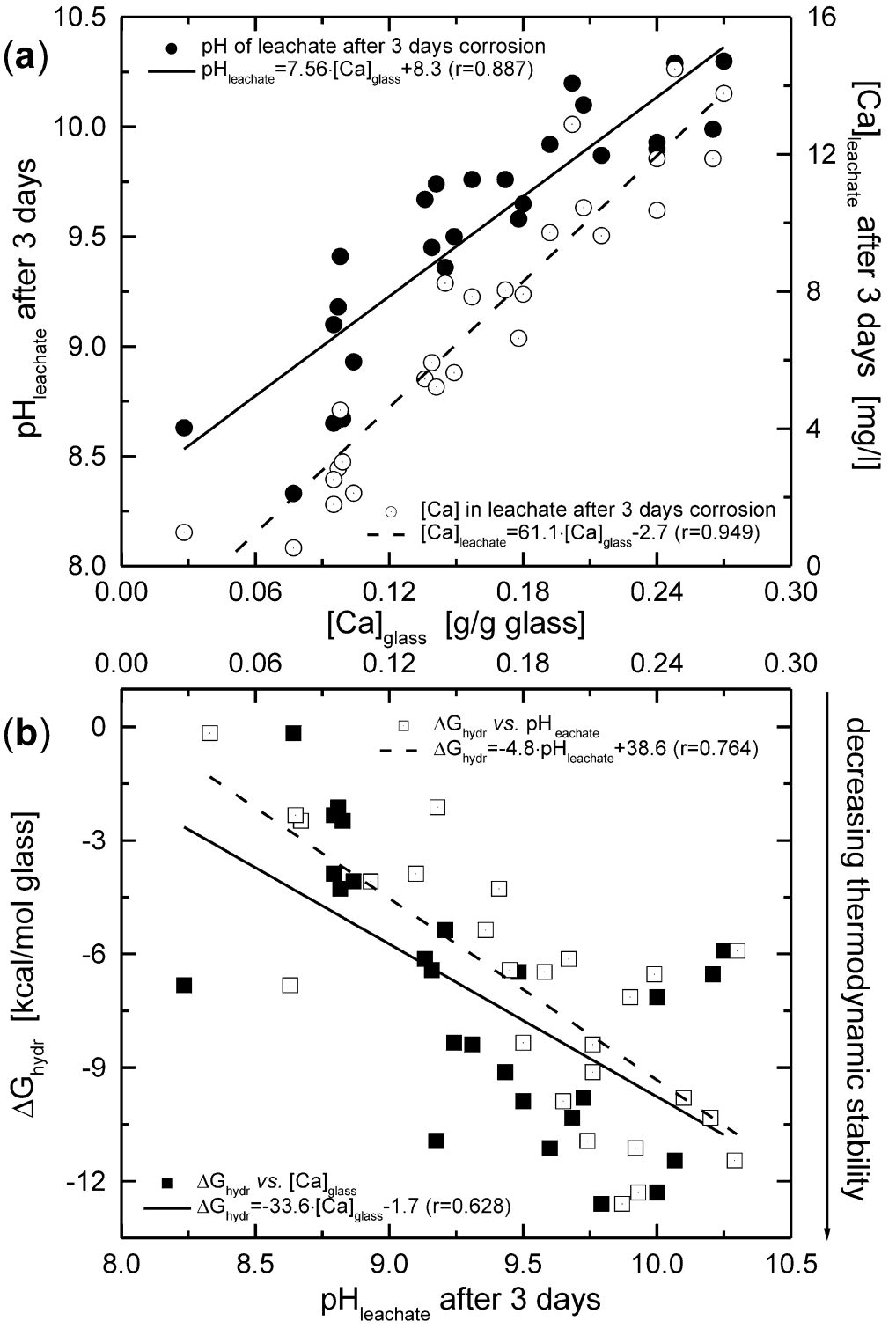

Fig. 5. (a) Relationships between the measured values of pH (solid circles; solid line) and Ca (doted circles; doted line) in the leachates of the 3-day corrosion test, and the proportion of Ca in the waste glasses and standards. (b) Relationships between the calculated free energy of hydration, and the proportion of Ca (solid squares; solid line) in waste glasses and standards, respectively the pH of the leachates (doted squares, doted line) after 3 days corrosion.

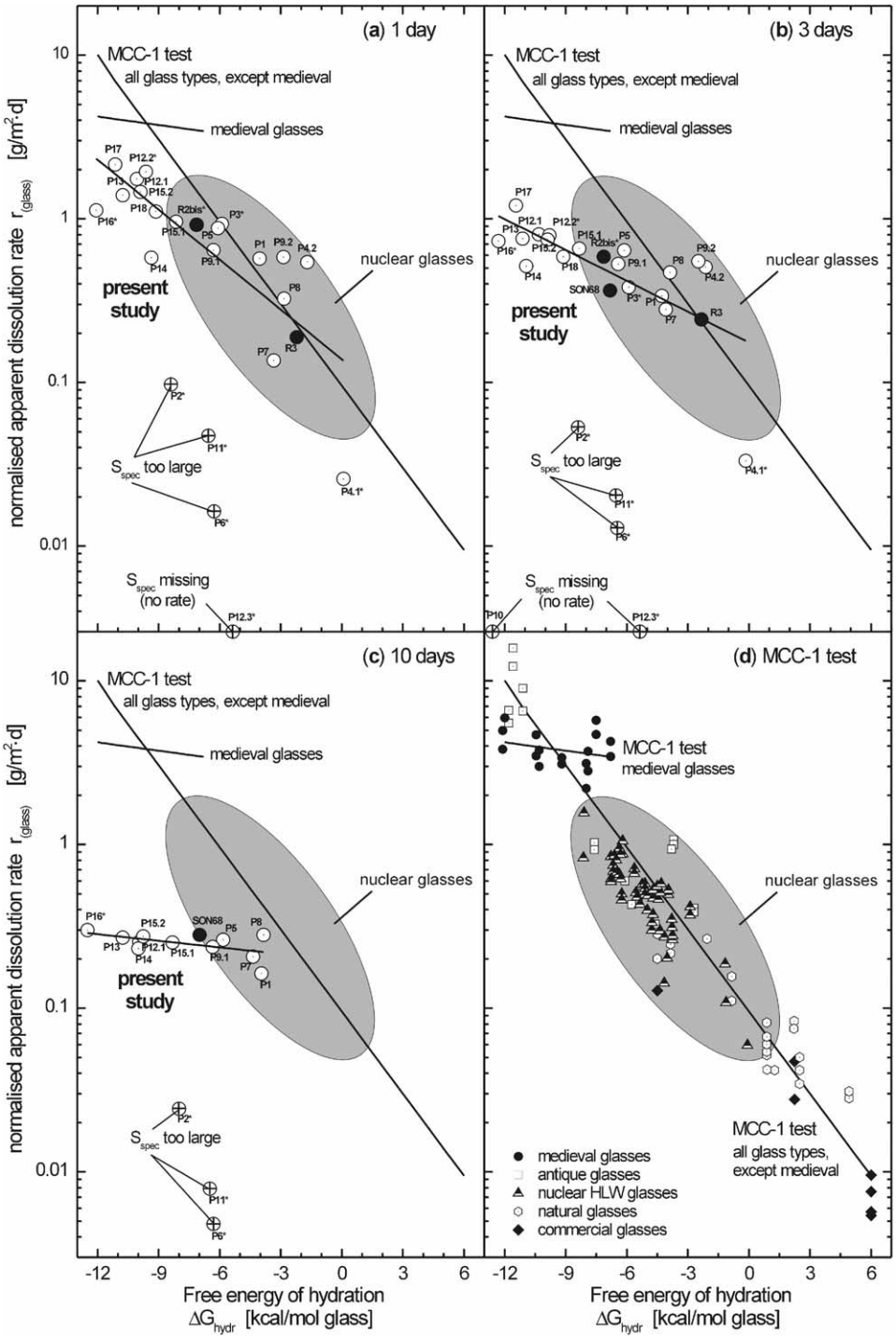

Fig. 6. Relationship between the normalised apparent dissolution rate of samples and the free energy of hydration. (a–c) Corrosion of waste glasses (dotted circles) and standards (solid circles) according to the conditions of the Strasbourg test (1-, 3- 10-day experiments; rates for 1 and 10 days are the average of the duplicate experiments). Crossed circles indicate data which were not taken into account to determine the correlation between r_{glass} and ΔG_{hydr}. (d) Literature-extracted (Plodinec and Wicks, 1994) relationship between the normalised apparent dissolution rate of glasses and the free energy of hydration for a set of 115 different glasses, according to the conditions of the MCC-1 test. The correlation for medieval glasses is different from that for the other glasses, and is plotted apart. Correlations obtained for the MCC-1 test (medieval glasses; other glasses) are reproduced in (a–c) for comparison.

dissolution rate, Fig. 6 shows that there is a fairly tight inverse relationship between the dissolution rate after 1 day corrosion, and the thermodynamic stability of the samples: a difference of ca. 10 kcal/mol between two samples results in an approximately one order of magnitude difference between their dissolution rates. This suggests that the simple thermodynamic approach may be used to gain information on the long-term stability of waste glasses. One can also notice that the points corresponding to the standard HLW glass SON68 corroded during 3 and 10 days are very close to literature data obtained for HLW glasses, indicating that the corrosion test yields results similar to the MCC-1 test for similar sample types. On the other hand, the effect of the differences in ΔG_{hydr} on the dissolution rates vanishes after 3–10 days, showing that the behaviour of glasses depends on the conditions of corrosion.

The most striking feature is the decrease in apparent rate obtained for 10-day corrosion (Fig. 6c), as compared to the steep initial increase obtained for 1-day corrosion (Fig. 6a). The results allow a clear differentiation of samples during the initial stage of matrix hydrolysis, and then evolve toward limited and uniform glass dissolution (ca. 0.25 $g/m^2 \times d$, calculated from Si releases over 10 days) when performed over long periods. This observation was also confirmed for other elements.

Although the $\Delta t \cdot S_{glass}/V_{leachant}$ is similar for the MCC-1 test (2.8 d/cm) and the Strasbourg test (0.2–2 d/cm), the technical discrepancy between the two corrosion tests (blocks *vs*. powder) complicates the comparison of the results to the literature data obtained by means of the MCC-1 test. Under the conditions of the MCC-1 test, block samples are allowed to react under a regime of initial corrosion, where differences in leaching rates r_0 can easily be highlighted between various glasses.

The difference in behaviour between the Strasbourg test and the MCC-1 test is probably explained by the fact that, in the former case, silicated secondary products are already formed after 3 days, leading to a regime of quasi-equilibrium and eventual scavenging of the previously dissolved silica.

The difference between the results of the MCC-1 test (Fig. 6d) obtained on medieval glasses (flat slope) and on the other glasses (steep slope) is not highlighted nor discussed in the seminal papers of Jantzen (1988), Plodinec (1984), Plodinec and Wicks (1994). This difference in behaviour between the two types of glasses is probably due to their different compositions. The medieval glasses are indeed richer in Mg, which favours the formation of protective secondary phases. It was shown for example by Thomassin and Touray (1979), Thomassin et al. (1985), and Crovisier et al. (1987) that brucite-like minerals ($Mg(OH)_2$) favour the fast formation of phyllosilicates from basaltic glasses. In fact, one can observe in Fig. 2 that the present samples contain Mg (ca. 1–3.8 wt.%), while this element is not present in the standard glass SON68, corroborating the preceeding assumption. Nevertheless, the pH-buffering conditions developed by the waste glasses during the course of corrosion (pH = 7–10.3) could also explain, at least partly, the non discriminating slope of $r_{(glass)} = f(\Delta G_{hydr})$ obtained after 10 days corrosion.

Thus, Fig. 6 makes it possible to distinguish several families of glasses for which the retention properties of heavy metals by secondary minerals are probably very different in short term corrosion, but this differentiation becomes negligible as corrosion processes toward longer term. Finally, the overall ΔG_{hydr} of the present waste glasses lies within the range of the thermodynamic stabilities of medieval, antique and nuclear HLW glasses.

4. Conclusion

One of the main aims of the physico-chemical characterisation of glasses produced for the immobilisation of domestic or nuclear wastes is the estimation of their long-term behaviour. It is expected that the durability of the studied materials reflects potentially low long-term release of toxic metals in the environment, especially if waste glasses are to be reused for civil engineering purposes. In that respect, domestic waste glasses inherit most of their final characteristics from the input wastes and residues from which they are produced. The results show that the overall quality of waste glasses is mostly dictated by the ratio between network-forming elements (mostly Si) and network-modifying elements (mostly Ca). The type of process (in-line processes; post-processes) used to produce these waste glasses plays a minor role on the chemical stability (element releases during corrosion) or thermodynamic stability (free energy of hydration), though post-processes for fly ash yield Ca-richer glasses, which may slightly impair their durability. Surprisingly, there are no differences in behaviour between vitreous and vitrocrystalline waste glasses.

The thermodynamic stability of the waste glasses studied spreads over a fairly large range (ca. 0 kcal/mol for the most favourable samples, to ca. −12 kcal/mol for the least favourable ones). Literature data show that the thermodynamic stability of medieval, antique and nuclear HLW glasses lies within this range. These intensively studied glasses may thus be considered as pertinent analogs of domestic waste glasses. While the observed durability of medieval and antique glasses is $\geqslant$1 ka (Gillies and Cox, 1988; Macquet and Thomassin, 1992; Sterpenich, 1998), the estimated durability of nuclear HLW glasses exceeds 10 ka (Jollivet et al., 1998). It is thus expected that the waste glasses studied will exhibit durabilities within the same order of magnitude.

The results of the thermodynamic approach provide valuable information for high-temperature process developers on one hand, and for waste management and environmental policy on the other hand. Calculations of ΔG_{hydr} show that changes to the final composition of waste glasses (e.g., more Si, Al, and in particular Mn; much less Ca) would drastically increase their overall stability, without impairing their ability to embed toxic metals. In that respect, in-line processes for MSW and post-processes for BA are better candidates for process optimisation, as their input materials (MSW, respectively BA) already contain relatively high proportions of Si and low proportions of Ca. With regard to the setup of environmental guidelines for the possible disposal or reuse of waste glasses, the results show that, whatever the thermodynamic stability of the samples studied, their releases of toxic metals under highly aggressive conditions of corrosion are systematically very low.

Acknowledgements

The authors are grateful to the companies which provided the samples (ABB, CT-Umwelttechnik, Küpat, Le Gaz Intégral, MGC-Plasma, Seiler, Steinmüller, Thermoselect, VonRoll Umwelttechnik) and the standards (CEA Marcoule, EDF Renardières) for this study. Pascale Colombel and Laurent Duffour (Prime-Verre, France) are acknowledged for fruitful discussions. Financial support was provided to DP, PS, GS and UM by the Swiss Agency for Environment, Forests and Landscape. B. Grambow and M.J. Plodinec reviewed the manuscript and suggested pertinent modifications.

References

Advocat, T., 1991. Les Mécanismes de Corrosion en Phase Aqueuse du Verre Nucléaire R7T7; Approche Expérimentale, Essai de Modélisation Thermodynamique et Cinétique. PhD dissertation, Univ. Louis Pasteur, Strasbourg.

Bates, J.K., Bradley, C.R., Buck, E.C., Cunnane, J.C., Ebert, W.L., Feng, X., Mazer, J.J., Wronkiewicz, D.J., Sproull, J., Bourcier, W.L., McGrail, B.P., Altenhofen, M.K., 1994. High-level Waste Borosilicate Glass: A Compendium of Corrosion Characteristics. Technical report DOE-EM-0177, US-DOE, Washington.

Cheron, P., Chevalier, Ph., Do Quang, R., Tanguy, G., Sourrouille, M., Woigner, S., Senoo, M., Banka, T., Kuramoto, K., Yamaguchi, T., Shimizu, K., Fillet, C., Jacquet-Francillon, N., Godard, J., Dussossoy, J.-L., Pacaud, F., Charbonnel, J.-G., 1995. Examination and testing of an active glass sample produced by COGEMA. In: Murakami, T., Ewing, R.C., (Eds.), Scientific Basis for Nuclear Waste Management XVIII. Mat. Res. Soc. Symp. Proc., vol. 353, pp. 55–62.

Colombel, P., 1996. Etude du Comportement à Long Terme de Vitrifiats de REFIOM. PhD dissertation, Univ. Poitiers, Poitiers.

Colombel, P., Godon, N., Vernaz, E., Thomassin, J.-H., 1997. Mécanismes d'altération des vitrifiats de REFIOM et analogie avec d'autres verres industriels ou naturels. In: Cases, J.-M., Thomas, F. (Eds.), Proc. Procédés Solidification Stabilisation Déchets. Nancy, pp. 450–454.

Crovisier, J.-L., Honnorez, J., Eberhart, J.-P., 1987. Dissolution of basaltic glass in seawater: mechanism and rate. Geochim. Cosmochim. Acta 51, 2977–2990.

Crovisier, J.-L., Honnorez, J., Fritz, B., Petit, J.-C., 1992a. Dissolution of subglacial basaltic glasses from Iceland: laboratory study and modelling. Appl. Geochem. Suppl. Issue 1, 55–81.

Crovisier, J.-L., Vernaz, E., Dussossoy, J-L., Caurel, J., 1992b. Early phyllosilicates formed by alteration of R7T7 glass in water at 250 °C. Appl. Clay Sci. 7, 47–57.

Ebert, W.L., Mazer, J.J., 1994. Laboratory testing of waste glass aqueous corrosion: effects of experimental parameters. In: Barkatt, A., Van Konynenbourg, R.A. (Eds.), Scientific Basis for Nuclear Waste Management XVII. Mater. Res. Soc. Symp. Vol. 333, pp. 27–40.

Ehret, G., Crovisier, J-L., Eberhart, J.-P., 1986. A new method for studying leached glasses: analytical electron microscopy on ultramicrotomic thin sections. J. Non-Cryst. Solids 86, 72–79.

Ewing, R.C., 1996. Glass as a Waste Form and Vitrification Technology: Summary of an international workshop. National Research Council, National Academy Press, Washington.

Fillet, S., 1987. Mécanismes de Corrosion et Comportement des Actinides dans le Verre Nucléaire R7T7. PhD dissertation, Univ. du Languedoc, Montpellier.

Gillies, K.J.S., Cox, G.A., 1988. Decay of medieval stained glass at York, Canterbury and Carlisle; II. Relationship between the composition of the glass, its durability and the weathering products. Glasstech. Ber. 61, 101–107.

Grambow, B., 1985. A general rate equation for nuclear waste glass corrosion. In: Jantzen, C.M., Stone, J.A., Ewing, R.C., (Eds.), Scientific Basis for Nuclear Waste Management VIII, Mater. Res. Soc. Symp. Proc. Vol. 44, pp. 16–27.

Grambow, B., 1994. Remaining uncertainties in predicting long-term performance of nuclear waste glass from experiments. In: Barkatt, A., Van Konynenbourg, R.A. (Eds.), Scientific Basis for Nuclear Waste Management XVII, Mater. Res. Soc. Symp. Vol. 333, pp. 167–180.

Grambow, B., Müller, R., 2001. First-order dissolution rate law and the role of surface layers in glass performance assessment. J. Nucl. Mater. 298, 112–124.

Grambow, B., Strachan, D.M., 1983. Leach testing of waste glasses under near-saturation conditions. In: Mc Vay, G.L. (Ed.), Scientific Basis for Nuclear Waste Management, Mater. Res. Soc. Symp. Proc. Vol. 26, pp. 623–634.

Jantzen, C.M., 1984. Effects of Eh (oxidation potential) on borosilicate waste glass durability. Adv. Ceram. 8, 385–393.

Jantzen, C.M., 1988. Prediction of glass durability as a function of glass composition and test conditions: thermodynamics and kinetics. In: Bickford, D.F., Boulos, E.N., Lingscheit, J.N., Olix, F., Horsfall, W.E., Woolley, F.E., Harding, F., LaCourse, W.C., Pye, L.D. (Eds.), Proc. 1st Int. Conf. Advances Fusion Glass. pp. 24.1–24.17.

Jantzen, C.M., Plodinec, M.J., 1984. Thermodynamic model of natural, medieval and nuclear waste glass durability. J. Non-Cryst. Solids 67, 207–223.

Jollivet, P., Nicolas, M., Vernaz, E., 1998. Estimating the alteration kinetics of the French vitrified high-level waste package in a geologic repository. Nucl. Technol. 123, 67–81.

Linard, Y., 2000. Détermination des Enthalpies Libres de Formation des Verres Borosilicatés; Application à l'Étude de l'Altération des Verres de Confinement de Déchets Radioactifs. PhD dissertation, Univ. Paris VII, Paris.

Macquet, C., Thomassin, J.H., 1992. Archaeological glasses as modelling of the behaviour of buried nuclear waste glasses. Appl. Clay Sci. 7, 17–31.

Malow, G., 1982. The mechanisms for hydrothermal leaching of nuclear waste glasses: properties and evaluation of surface layers. In: Lutze, W. (Ed.), Scientific Basis for Nuclear Waste Management V, Mater. Res. Soc. Symp. Proc. Vol. 11, pp. 25–36.

Newton, R.G., 1985. The durability of glass. Glass Technol. 26, 21–38.

Newton, R.G., Paul, A., 1980. A new approach to predicting the durability of glasses from their chemical compositions. Glass Technol. 21, 307–309.

Nogues, J.-L., 1984. Les Mécanismes de Corrosion des Verres de Confinement des Produits de Fission. PhD dissertation, Université de Montpellier II, Montpellier.

Oelkers, E.H., 2001. General kinetic description of multioxide silicate mineral and glass dissolution. Geochim. Cosmochim. Acta 65, 3703–3719.

Oelkers, E.H., Gislason, S.R., 2001. The mechanism, rates and consequences of basaltic glass dissolution: I. An experimental study of the dissolution rates of basaltic glass as a function of aqueous Al, Si and oxalic acid concentration at 25 °C and pH = 3 and 11. Geochim. Cosmochim. Acta 65, 3671–3681.

Paul, A., 1977. Chemical durability of glasses. J. Mater. Sci. 12, 2246–2268.

Paul, A., 1982. Chemistry of Glasses. Chapman and Hall, London.

Perret, D., Stille, P., Shields, G., Crovisier, J.-L., Mäder, U., 2000. Long-term Stability of HT Material. Techical Report #4. Swiss Agency for Environment, Forests and Landscape, Bern. (also available as a CD-ROM with appendices from SAEFL, Division Waste).

Petit, J.-C., Della Mea, G., Dran, J.-C., Magonthier, M.-C., Mando, P.A., Paccagnella, A., 1990. Hydrated layer formation during dissolution of complex silicate glasses and minerals. Geochim. Cosmochim. Acta 54, 1941–1955.

Plodinec, M.J., 1984. Stability of radioactive waste glasses assessed from hydration thermodynamics. In: McVay, G.L. (Ed.), Scientific Basis for Nuclear Waste Management VII, Mater. Res. Soc. Symp. Proc. Vol. 26, pp. 755–762.

Plodinec, M.J., Wicks, G.G. 1994. Application of hydration thermodynamics to in-situ test results. In: Barkatt, A., Van Konynenbourg, R.A. (Eds.). Scientific Basis for Nuclear Waste Management XVII, Mater. Res. Soc. Symp. Proc. Vol. 333, pp. 145–157.

Scholze, H., 1991. Glass, Nature, Structure, and Properties. Springer-Verlag, New York.

Sproull, J.F., Marra, S.L., Jantzen, C.M., 1994. High-level radioactive waste glass production and product description. In: Barkatt, A., Van Konynenbourg, R.A. (Eds.), Scientific Basis for Nuclear Waste Management XVII, Mater. Res. Soc. Symp. Proc. Vol. 333, pp. 15–25.

Sterpenich, J. (1998). Altération des vitraux médiévaux, contribution à l'étude du comportement à long terme des verres de confinement. PhD dissertation, Univ. Henri Poincaré, Nancy.

Swiss Agency for Environment, Forests and Landscape (SAEFL), 1996. TVA/OTD: Technische Verordnung über Abfälle/Ordonnance sur le Traitement des Déchets. #814.015. SAEFL, Bern, Switzerland.

Swiss Agency for Environment, Forests and Landscape (SAEFL), 1998. GSchV/OEaux: Gewässerschutzverordnung /Ordonnance sur la Protection des Eaux. #814.210. SAEFL, Bern, Switzerland.

Thomassin, J.-H., Touray, J.-C., 1979. Etude des premiers stades de l'interaction eau-verre basaltique: données de la spectrométrie de photoélectrons (XPS) et de la microscopie électronique à balayage. Bull. Minéral 102, 594–599.

Thomassin, J.-H., Crovisier, J.-L., Touray, J.-C., Juteau, T., Boutonnat, F., 1985. L'apport de la géochimie expérimentale à la compréhension des interactions eau de mer- verre basaltique entre 3 et 90 °C: données de l'analyse ESCA, de la microscopie et de la micro diffraction électroniques. Bull. Soc. Géol. Fr. 2, 217–222.

Vernaz, E., Advocat, T., Dussosoy, J.-L., 1990. Effects of the Sa/V ratio on the long-term corrosion kinetics of R7T7 glass. Nuclear Waste Management III, Ceram. Trans. 9, 175–185.

Vernaz, E., Dussosoy, J.-L., 1992. Current state knowledge of nuclear waste glass corrosion mechanisms: the case of R7T7 glass. Appl. Geochem. Suppl. Issue 1, 13–22.